Cellular Signalling 64 (2019) 109391

Contents lists available at ScienceDirect

Cellular Signalling

journal homepage: www.elsevier.com/locate/cellsig

MicroRNA-6077 enhances the sensitivity of patients-derived lung adenocarcinoma cells to anlotinib by repressing the activation of glucose transporter 1 pathway

De-bin Ma[a], Meng-meng Qin[a], Liang Shi[a,*], Xin-min Ding[b,*]

[a] Department of Respiratory and Critical Care Medicine, General Hospital of Northern Theater Command, Shenyang 110016, China
[b] Department of Respiratory and Critical Care Medicine, Beijing Shijitan Hospital affiliated to Capital Medical University, Beijing 100038, China

ARTICLE INFO

Keywords:
miR-6077
GLUT1
Patient-derived cell lines
Lung adenocarcinoma
Anlotinib

ABSTRACT

Anlotinib is a novel molecular targeted agent targeting the vascular endothelial growth factor receptor, which differs from the other currently available non-small cell lung cancer (NSCLC) molecular targeted drugs targeting this receptor. Although the application of anlotinib may bring new hope for patients with advanced NSCLC, the cost of treatment is high. The results of this study showed that microRNA-6077 (miR-6077) represses the expression of GLUT1 (glucose transporter 1) and enhances the sensitivity of patient-derived lung adenocarcinoma (AC) cells to anlotinib. The miR-6077, which potentially binds to the 3'untranslated region of GLUT1, was identified and screened by miRDB, an online tool; sequences of miR-6077 were prepared as lentivirus particles. A549 cells (a lung adenocarcinoma cell line) and five patient-derived AC cell lines were infected with control miRNA or miR-6077, and subsequently treated with the indicated concentration of anlotinib. The expression of proteins, such as GLUT1, was determined by western blotting. The antitumor effect of anlotinib was identified through in-vitro (e.g., MTT) or in-vivo methods (e.g., subcutaneous tumor model). Overexpression of miR-6077 repressed the expression of GLUT1 and decreased the glucose uptake, lactate production, or ATP generation in AC cells. In addition, MiR-6077 may enhance the antitumor effect of anlotinib on A549 or patient-derived AC cell lines. Therefore, our results indicated that miR-6077 represses the expression of GLUT1 and enhances the sensitivity of patients-derived lung AC cells to anlotinib.

1. Introduction

Lung cancer is one of the most common human cancers and a serious threat to human health [1–3]. Due to the limitation of current technologies applied to clinical diagnosis, a large number of patients are suffering from an advanced stage of disease (advanced lung cancer) even at initial diagnosis. Therefore, surgical operation may not be suitable, and the prognosis or clinical outcome of patients with advanced lung cancer is poor [4–6]. Clinical strategies for the treatment of advanced lung cancer are great challenges for doctors or researchers in related fields. Molecular targeting agents, such as gefitinib or erlotinib, which were developed to target the endothelial growth factor receptor (EGFR), have been widely used and demonstrated clear therapeutic effects [7–9]. However, during the treatment, patients often develop tolerance to drugs due to multiple factors, such as EGFR mutation [10,11]. To resolve this problem, new molecular targeting agents targeting the vascular EGFR (VEGFR), such as anlotinib, have been developed and provide new hope for patients with lung cancer [12–14]. Achieving safer and more effective molecular targeted therapy is of great importance.

It is established that the metabolism of human cancer cells increases to adapt to the rapid proliferation or aggressive metastasis of cancer cells [15,16]. The increasing metabolism, termed "the Warburg effect", is featured by an elevated glucose uptake, which is mediated by the glucose transporter proteins (GLUTs), and the lactic fermentation of glucose even at the aerobic condition [17,18]. Among GLUTs, glucose transporter 1 (GLUT1), which is encoded by the solute carrier family 2 gene (SLC2A1), is overexpressed in human cancers and participates in the progression or metastasis of cancer cells [19–21]. Moreover, the effects of lactic fermentation of the Warburg effect on the alteration of the microenvironment of tumor tissues enhancing the metastasis or the resistance to antitumor drug have attracted the attention of researchers. Therefore, inhibiting the expression or activation of GLUT1 is a promising strategy for the treatment of human cancer.

* Corresponding authors.
E-mail addresses: shiliang188@163.com (L. Shi), dingfirst@sina.com (X.-m. Ding).

https://doi.org/10.1016/j.cellsig.2019.109391
Received 1 August 2019; Received in revised form 10 August 2019; Accepted 13 August 2019
Available online 14 August 2019

Anlotinib is a newly approved molecular targeted agent for the treatment of non-small cell lung cancer (NSCLC), especially lung adenocarcinoma (AC), the most common subtype of lung cancer [22–24]. Anlotinib targets the VEGFR-related signaling pathway, and inhibits the proliferation or metastasis of AC cells [13,25]. At present, the cost of anlotinib continues to bring tremendous financial burden on NSCLC patients. The discovery and establishment of an anlotinib sensitization strategy may assist in improving the therapeutic effect of anlotinib and achieving a similar antitumor effect through reduced dosage. It can also avoid or improve the potential toxic side effects caused by drug treatment and help to alleviate the economic burden of patients. In the present study, the full-length sequences of microRNA 6077 (miR-6077) were prepared as lentivirus particles to overexpress miR-6077 in A549, a typical AC cell line, or patient-derived AC cell (PDC) lines. The influence of miR-6077 on the antitumor effect of anlotinib on AC cells was examined using in-vitro or in-vivo methods. The results showed that miR-6077 repressed the expression of GLUT1 and enhanced the sensitivity of PDCs to anlotinib.

2. Materials and methods

2.1. Cell line and agents

The lung AC cell lines A549 or PDC lines were preserved in our laboratory [26]. The lentivirus containing the full-length sequence of miR-6077, GLUT1, or GLUT1 with mutated miR-6077-binding sites was constructed by Vigene Corporation (Jinan, China). The vectors of GLUT1 with mutated miR-6077-binding sites were named as $GLUT1^{Mut}$. The inhibitor of miR-6077 was purchased from Thermo Fisher Scientific Corporation (Waltham, MA, USA).

2.2. Clinical specimens and quantitative polymerase chain reaction (qPCR) experiment

The collection of clinical specimens (30-paired AC tissues and non-tumor tissues) was performed after obtaining written informed consent by the patients and approval by the Ethic Committee of the General Hospital of Northern Theater Command, Chinese People's Liberation Army. Total RNA samples from the clinical specimens or AC cells were extracted using a PARISTM Kit (Thermo Fisher Scientific), and the reverse transcription of RNA samples was performed using Multiscribe™ Reverse Transcriptase (Thermo Fisher Scientific Corporation). The qPCR experiment was performed according to the methods provided by Liang et al. and Ji et al. [27,28]. The primers used in the qPCR experiments are listed in Table 1.

2.3. Ion AmpliSeq targeted sequencing experiments [29,30]

The primers for GLUT1, GLUT2, GLUT3, GLUT4, GLUT5, GLUT6, GLUT7, GLUT8, GLUT9, GLUT10, GLUT11, or GLUT12 (the gene symbol of GLUT1～12 was SLC2A1, SLC2A2, SLC2A3, SLC2A4, SLC2A5, SLC2A6, SLC2A7, SLC2A8, SLC2A9, SLC2A10, SLC2A11 or SLC2A12) were designed using the online tool Ion AmpliSeq Designer (Thermo Fisher Scientific Corporation). Total RNA samples were extracted from the clinical specimens using RNA-extraction Kits (Applied Biosystems instruments; Thermo Fisher Scientific Corporation), and subjected to reverse transcription into cDNA using RNeasy Mini Kits (Qiagen, Valencia, CA, USA). The construction of a cDNA sample library was achieved using the Ion AmpliSeq Library Kits and the Ion Xpress Barcode Adapter reagents (Thermo Fisher Scientific Corporation). The examination panel of GLUTs was amplified using 2 × primer pool-buffers with a 25-cycle amplification (Ion Personal Genome Machine [PGM] Hi-Q View Sequencing Kit, Catalog number: A30044; Thermo Fisher Scientific Corporation). The Ion PGM Hi-Q sequencing kits and the Ion Torrent 318 chips (Ion 318 Chip Kit v2 BC, Catalog number: 4488150; Thermo Fisher Scientific Corporation) were used for the sequencing analysis through the Ion Torrent PGM platform (Ion PGM System, Catalog number: 4462921, Thermo Fisher Scientific Corporation). The Ion Torrent data were analyzed using the Ion Torrent Suite v3.0 software (Thermo Fisher Scientific Corporation). The primers were listed as Table 1.

2.4. Preparation of anlotinib formulation

The molecular agent anlotinib (Cat., No.: S8726) was purchased from Selleck Corporation (Houston, TX, USA). For cell-based experiments, anlotinib was dissolved using organic solvents (i.e., dimethyl sulfoxide [DMSO]), and subsequently diluted into indicated concentrations of resolutions by Dulbecco's Modified Eagle Medium [31]. The concentrations of anlotinib used in the cell-survival experiments were: 10 μmol/L, 3 μmol/L, 1 μmol/L, 0.3 μmol/L, 0.1 μmol/L, 0.03 μmol/L, or 0.01 μmol/L. For the animal experiments, 20 mg of apatinib was firstly dissolved in 100 μL DMSO, 200 μL polyethylene glycol 400, and 200 μL Tween 80 [32,33]. Subsequently, the solutions were slowly and carefully diluted using physiological saline to a solution with a total volume of 10 mL. During the dilution, the solution can be subjected to ultrasonic or churning treatment to improve the dissolution of the drug. The final concentration of DMSO, polyethylene glycol 400, or Tween 80 was no > 1‰, 2‰, or 2‰.

2.5. Cell culture and cell-survival examination

A549 and PDCs were cultured in Dulbecco's Modified Eagle Medium with 10% fetal bovine serum at 37 °C and 5% carbon dioxide condition. Cells infected with lentivirus particles were seeded into 96-well plates (8000 cells per well). Subsequently, the cells were treated with the indicated concentration of anlotinib for 48 h. After treatment, the cells were analyzed through MTT assays as previously described [29]. The

Table 1
The primers used in Ion AmpliSeq Targeted Sequencing experiments.

Gene Symbol	Pool	Ion_AmpliSeq_Fwd_Primer*	Ion_AmpliSeq_Rev_Primer*
SLC2A1	Pool1	GGCATGATTGGCTCCTTCTCT	GCCCAGGATCAGCATCTCAAA
SLC2A2	Pool1	CCTAGGCAGAGCTGCGAATA	CACAGCAGTGATGACAGTGAAAA
SLC2A3	Pool1	TGGAATCACCCCTAGATCTTTCTTGA	GGAGCATTGATGACCCCAGTG
SLC2A4	Pool1	TTTCTCCAACTGGACGAGCAA	GGCCTCGAGTTTCAGGTACT
SLC2A5	Pool1	GTAACCGTGTCCATGTTTCCATTTG	CGACTCTGCTGCATCCCATT
SLC2A6	Pool1	TGGTCTACACATCCCCTGTCA	GGAGGTCGTTGAGGATCATGG
SLC2A7	Pool1	ACATCGCGGGACATTCCATT	TGGATGGGAACAGGAAGCCTAT
SLC2A8	Pool1	GTCTCTGCACAGCCTGTTGAT	CCCTTGACATGCAGAGGGAA
SLC2A9	Pool1	AAAGATCCCATACGTCACCTTGAG	TGATGGTGAGGGTCCCAAAGA
SLC2A10	Pool1	CCTTCCTGCTCTACGGACTGA	AGTTCTGCCTGTGGCCAAA
SLC2A11	Pool1	GAGATGATCATGCTGGGAAGACT	ACGATCCCCAGAGCCGTAA
SLC2A12	Pool1	TCCTTAGCCAGCTTGCTTGT	GAGGAGATTGATGCCCCAGTT

Abbreviations: SLC2: solute carrier family 2; Fwd: forward; Rev.: Reverse;

relative number of cells in each group was examined by the optical density (OD) values at a wavelength of 490 nm. The inhibition rate of anlotinib on AC cells was calculated as follows: (Control group OD 490 nm − administration group OD 490 nm) / (Control group OD 490 nm) × 100%.

2.6. Antibodies and western blotting analysis

Antibodies against GLUT1, E-cadherin, N-cadherin, Vimentin, LDHA, and β-Actin were purchased from Abcam Corporation, Cambridge, UK. The protein levels of GLUT1, E-cadherin, N-cadherin, Vimentin, LDHA, and β-Actin were examined through western blotting using specific antibodies. The western blotting experiments were performed according to the method described by Li et al. [16]. The β-Actin was selected as the loading control. The images of western blot was quantitatively analyzed by Image J (National Institutes of Health, Bethesda, Maryland, USA), an Image analysis software, and the quantitative expression level of proteins were examined as the band-intensity. The inhibition rates were calculated as [(band-intensity of the control group) − (band-intensity of the administrated group)] / (band-intensity of the control group) * 100%.

2.7. Biochemical examination experiments

The biochemical examination experiments were carried out following the methods descripted by Li et al. 2017 [34]. The AC cells were collected and the effects of miR-6077 on cells', glucose uptake, lactate production and ATP generation were examined. On this basis, the inhibition rate was calculated: (control group biochemical index - experimental group biochemical index) / (control group biochemical index) * 100%.

2.8. Subcutaneous growth of AC cells in nude mice

All the protocols and methods of the animal experiments were approved by the Animal Care and Use Committee of General Hospital of Northern Theater Command, Chinese People's Liberation Army. All animal experiments were performed in accordance with the UK Animals (Scientific Procedures) Act, 1986 and associated guidelines. AC cells (A549 or PDCs) transfected with vectors were injected into nude mice to form subcutaneous tumors as previously described [35,36]. Following injection (7–10 days), the mice received solvent control or oral treatment with anlotinib at the indicated concentration every 2 days. After 3 weeks of treatment (i.e., 10 administrations), all nude mice were sacrificed, and the final volume and weight of subcutaneous tumors were measured [35,36].

2.9. The intrahepatic growth of AC cells in nude mice

For the liver migration experiments, A549 cells infected with vectors were injected into the livers of nude mice via the hepatic portal vein. The nude mice (4–5 weeks old) were purchased from Si-Bei-Fu Corporation (Beijing, China). Following injection (4–5 days), the mice received treatment with the indicated concentration of anlotinib once every 2 days. After 3 weeks of treatment (approximately 21 days/10 administrations), all mice were examined using microPET (Philips Corp., Netherlands) as described by Xu et al. and Zhang et al. [16,33]. After the microPET analysis, nude mice were harvested, and images of livers with lesions/nodules formed by A549 cells were obtained. Lesions/nodules formed by A549 cells in the livers of nude mice were quantitatively analyzed by measuring the radio-activation [37,38] of livers or the area of lesions/nodules according to the methods described by Xie et al. [33].

For the liver invasion experiments, A549 cells transfected with the indicated vectors were mixed with the biological–medical hydrogel (Cai-Hong-Yi-Xue-She-Bei Corporation, Kunming, China) to form hydrogel droplets. Subsequently, the hydrogel containing A549 cells was adhered onto the surface of the lives of nude mice. Mice were received oral administration of anlotinib once per 2 days. After 3 weeks of treatment (approximately 21 days/10 administrations), the mice were screening through microPET. The tumor nodules formed by the invasive growth of A549 cells were examined through Masson staining of the livers of nude mice following the methods described by Meng et al. [39]. The captured images were quantitatively analyzed to determine the relative invasive growth of A549 cells into the liver using the Image J software, as previously described [40]. The thickness of the nodules or the whole liver was quantitatively analyzed. The relative invasive growth of A549 cells in the liver (i.e., the thickness of nodules to the thickness of the liver) was calculated using the following formula: (nodule thickness in the control group)/(liver thickness in the control group) × 100% or (nodule thickness in the experimental group)/(liver thickness in the experimental group) × 100%. The inhibition rate in each group was calculated as follows: [(relative invasive growth in the control group) − (relative invasive growth in the experimental group)]/(relative invasive growth in the control group) × 100% [35]. Values were corrected for protein concentration and presented as the mean ± SD of replicate experiments [19,41,42].

2.10. Statistical analysis

The statistical analysis was performed by Bonferroni's correction without two-way analysis of variance using the SPSS statistical software (SPSS 9.0; IBM Corporation, Armonk, NY, USA). The IC_{50} value/concentration of anlotinib was calculated using the Origin software (Origin 6.1; OriginLab Corporation, Northampton, MA, USA). A $P < .05$ denoted statistical significance.

3. Results

3.1. miR-6077 is a miRNA potentially targeting the 3'untranslated region (3'UTR) of GLUT1

The expression of all GLUTS (GLUT1–12) was firstly examined in 30 pairs of clinical specimens (one AC and one non-cancer as a pair of tissues) from patients with the AC type of NSCLC. As shown in Fig. 1, the expression of GLUT1 in AC was markedly higher than that observed in non-tumor tissue (Fig. 1A). Moreover, in AC tissues, the expression level of GLUT1 is markedly higher than that of other GLUTs (Fig. 1B–M). Subsequently, miRDB (an online database) was used to predict a miR that potentially binds to the 3'UTR of GLUT1. The results are shown in Fig. 2; miR-6077 was shown to bind to the 3'UTR of GLUT1. The expression levels of GLUT1 and miR-6077 were also examined in clinical specimens to validate this finding. As shown in Fig. 2B–E, the expression of miR-3174 was negatively associated with that of GLUT1 in clinical samples. Moreover, western blotting analysis was performed to examine the effect of miR-6077 on the expression of GLUT1 in A549 cells (Fig. 2B). As shown in Fig. 2F and G, overexpression of miR-6077 repressed the expression of GLUT1. In addition, transfection with an inhibitor of miR-6077 or GLUT1 with mutated miR-6077-targeting sites ($GLUT1^{Mut}$) almost fully blocked the effect of miR-6077 (Fig. 2F, G). Therefore, miR-6077 is a miRNA targeting GLUT1.

3.2. Overexpression of miR-6077 enhanced the sensitivity of AC cells to anlotinib

Subsequently, the influence of miR-6077 on the antitumor effect of anlotinib was examined. As shown in Table 2, anlotinib may inhibit the survival of AC cells in a dose-dependent manner. Overexpression of miR-6077 enhances the sensitivity of AC cells to anlotinib, and the half maximal inhibitory concentration (IC_{50}) values of anlotinib on AC cells were decreased (Table 2). The expression of GLUT1 in A549 cells and

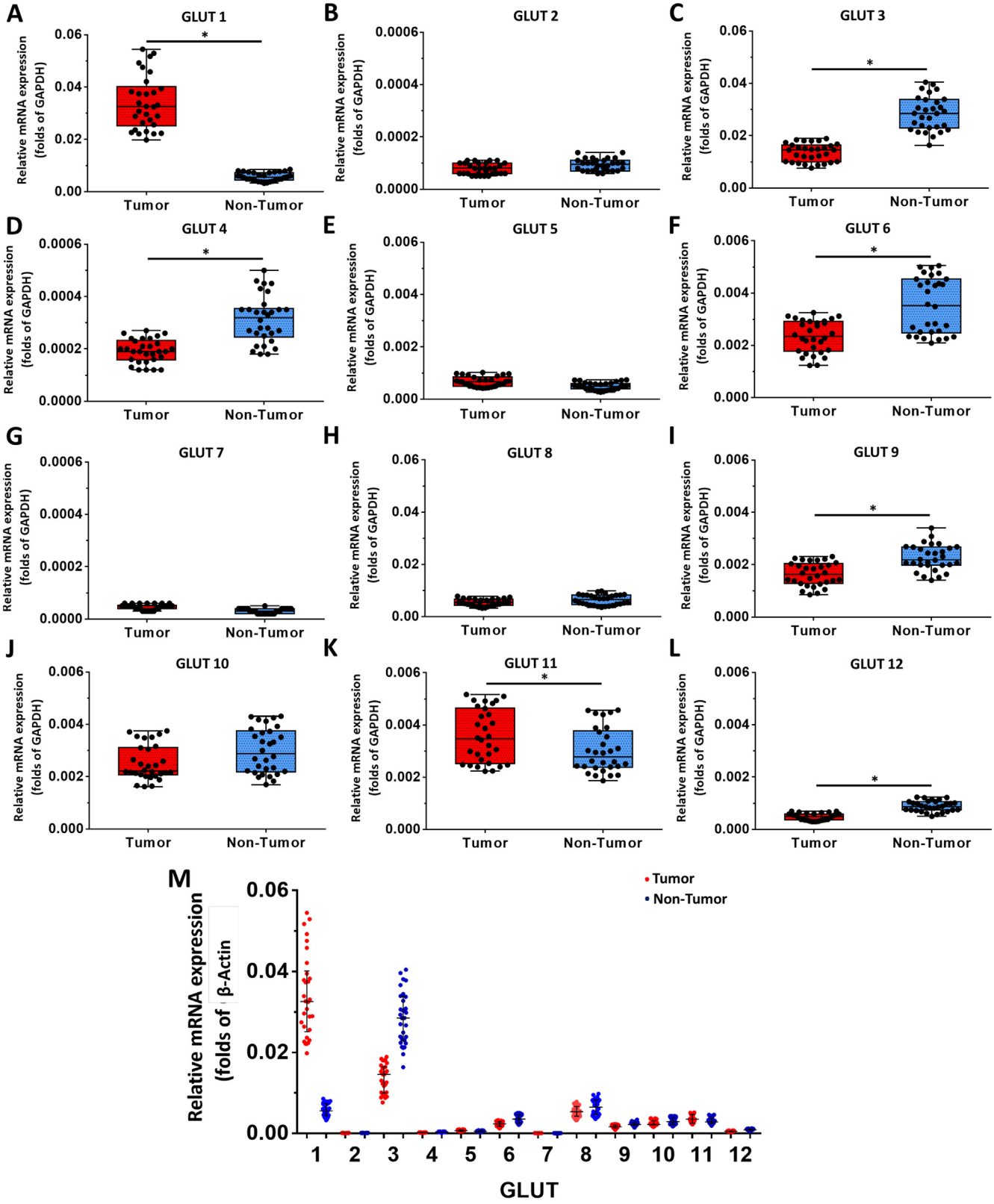

Fig. 1. The expression of GLUTs in clinical specimens obtained from AC patients. Total mRNA was extracted from 30 pairs of clinical specimens (AC and non-tumor tissues from the same patients). The expression levels of GLUT1 (A), GLUT2 (B), GLUT3 (C), GLUT4 (D), GLUT5 (E), GLUT6 (F), GLUT7 (G), GLUT8 (H), GLUT9 (I), GLUT10 (J), GLUT11 (K), and GLUT12 (L) were examined through AmpliSeq methods, and the results are shown as scatter diagrams. The expression levels of these 12 GLUTS are shown as a scatter diagram at the same coordinate (M). *P < .05.

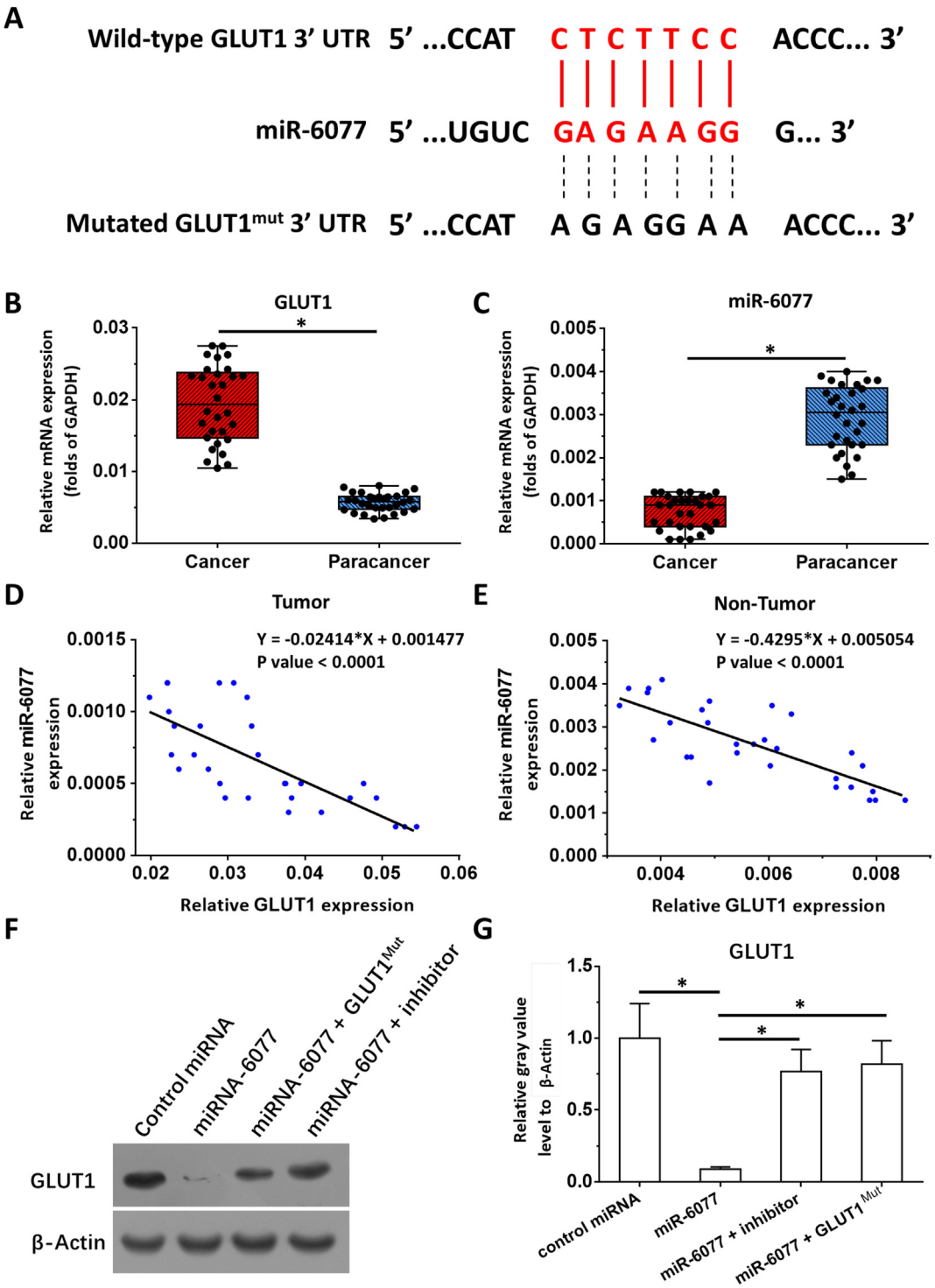

Fig. 2. miR-6077 is a microRNA targeting the 3'UTR of GLUT1. (A) miR-6077 was identified using an online tool (miRDB) and potentially targets the 3'UTR of GLUT1. The binding site and mutated binding site are shown as a schematic diagram. (B and C) The expression level of miR-6077 and the GLUT1 in tumor tissues or non-tumor tissues are shown as a scatter plot. (D and E) The relationship between the expression level of miR-6077 and the GLUT1 in tumor tissues (D) or non-tumor tissues (E) is shown as a scatter plot. (F and G) A549 cells transfected with control miRNA, miR-6077, miR-6077 + GLUT-1Mut, or miR-6077 + inhibitor of miR-6077 were harvested for western blotting analysis. The results are shown as images of western blotting (F) or quantitative analysis (G). *$P < .05$.

PDCs was shown in Supplemental Fig. 1. Moreover, transfection with an inhibitor of miR-6077 or GLUT1^{Mut} inhibited the effect of miR-6077 on AC cells (Table 2). Western blotting was performed to further examine the effect of miR-6077 on AC cells. As shown in Fig. 3, miR-6077 decreased the expression of N-cadherin or Vimentin, two mesenchymal indicators, and enhanced the expression of E-cadherin, an epithelial indicator. Overexpression of miR-6077 also inhibited the expression of GLUT-1 and lactate dehydrogenase A (LDHA) in A549 cells. Similar results were obtained in PDCs cells (Supplemental Table 1). Furthermore, the effect of miR-6077 on the glucose uptake, lactate production, or ATP generation in AC cells was shown as Table 3: overexpression of miR-6077 inhibited the glucose uptake, lactate production, or ATP generation in AC cells and transfection of GLUT1^{Mut} or miR-6077's inhibitor decreased the effect of miR-6077. Therefore, miR-6077

Table 2
The IC_{50} values of anlotinib on AC cells' survival.

Cell lines	control miRNA	miR-6077	miR-6077 + GLUT1^{Mut}	miR-6077 + inhibitor
	IC_{50} values (μmol/L) of anlotinib			
A549	0.59 ± 0.08	0.10 ± 0.03	0.61 ± 0.10	0.52 ± 0.07
AC PDCs No. 1	0.99 ± 0.16	0.31 ± 0.46	1.15 ± 0.59	0.95 ± 0.25
AC PDCs No. 2	0.77 ± 0.11	0.20 ± 0.05	0.78 ± 0.36	0.70 ± 0.03
AC PDCs No. 3	1.85 ± 0.29	0.33 ± 0.08	1.10 ± 0.38	1.29 ± 0.49
AC PDCs No. 4	1.054 ± 0.74	0.58 ± 0.10	1.38 ± 0.70	1.28 ± 0.47
AC PDCs No. 5	0.74 ± 0.24	0.10 ± 0.04	0.63 ± 0.06	0.49 ± 0.35

Abbreviations: PDCs: patients-derived cells; AC: Lung adenocarcinoma; IC_{50}: half maximal inhibitory concentration.

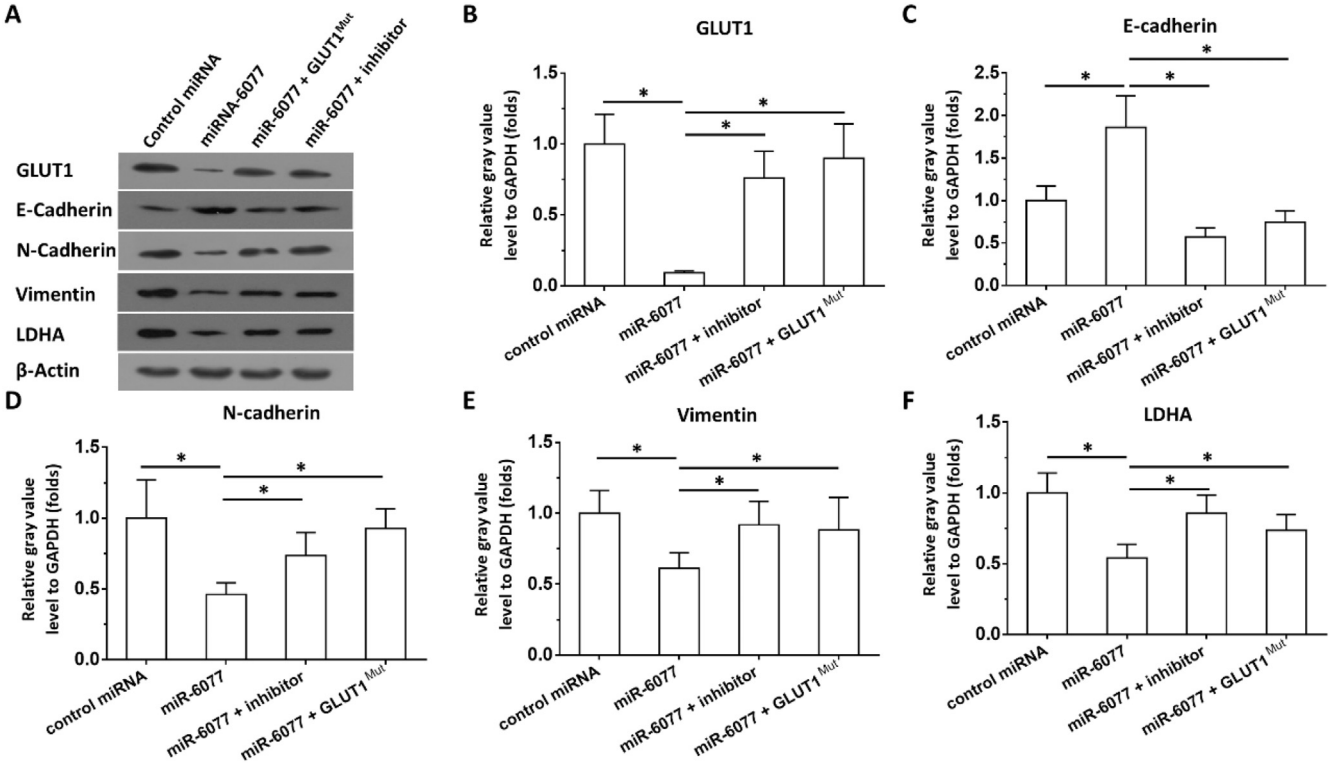

Fig. 3. miR-6077 decreased the EMT and expression of genes related to the Warburg effect in A549 cells. A549 cells transfected with control miRNA, miR-6077, miR-6077 + GLUT-1Mut, or miR-6077 + inhibitor of miR-6077 were harvested for western blotting analysis. The results are shown as images of western blotting (A) or quantitative analysis (B–F). *P < .05.

inhibited the epithelial-mesenchymal transition process and the expression of genes related to the Warburg effect in AC cells by repressing the expression of GLUT1. Overexpression of miR-6077 also inhibited the glucose uptake, lactate production, or ATP generation in AC cells.

3.3. Overexpression of miR-6077 enhanced the antitumor effect of anlotinib on the subcutaneous growth of AC cells

Subsequently, the in-vivo antitumor effect of anlotinib on AC cells was examined using a subcutaneous tumor model. As shown in Fig. 4 and Table 4, oral administration of anlotinib inhibited the subcutaneous growth of AC cells in nude mice. Overexpression of miR-6077 enhanced the sensitivity of AC cells to anlotinib. To further examine the specificity of miR-6077 for AC cells, the cells were transfected with GLUT1Mut. As shown in Fig. 5 and Table 4, transfection with GLUT1^{Mut} almost blocked the effect of miR-6077 on the antitumor property of anlotinib. Therefore, overexpression of miR-6077 enhanced the antitumor effect of anlotinib on the subcutaneous growth of AC cells by targeting GLUT1.

3.4. Overexpression of miR-6077 enhanced the antitumor effect of anlotinib on the intrahepatic growth of AC cells

To further examine the in-vivo antitumor activation of anlotinib, the intrahepatic growth of AC cells in nude mice, mimicking the lung cancer-liver metastasis or invasion, was also determined. AC cells were injected into the livers of nude mice via a hepatic portal vein injection to mimic the migration of AC cells. As shown in Fig. 6, A549 cells formed multiple and diffuse lesions in the liver. The results are shown as images of micro positron emission tomography (microPET) or livers with lesions. Oral administration of anlotinib inhibited the formation of lesions by A549 cells in the livers of nude mice. Overexpression of miR-6077 enhanced the antitumor effect of anlotinib on the formation of lesions by A549 cells in nude mice (Fig. 6). Transfection with GLUT1^{Mut} almost blocked the effect of miR-6077. Similar results were obtained from the intrahepatic invasion experiments (Fig. 7). Therefore, overexpression of miR-6077 enhanced the sensitivity of A549 cells to anlotinib.

Table 3
The inhibition rates (%) of anlotinib on AC cells' glucose uptake, lactate production or ATP generation.

Cell lines		Control miRNA	miR-6077	miR-6077 + GLUT1^{Mut}	miR-6077 + inhibitor
		The inhibition rates (%) of anlotinib			
A549	glucose uptake	–	62.19 ± 4.82	9.31 ± 5.70	19.69 ± 1.89
	lactate production	–	49.59 ± 5.41	5.44 ± 0.74	10.90 ± 0.86
	ATP generation	–	58.17 ± 2.45	–	–
AC PDCs No. 1	glucose uptake	–	41.2 ± 3.35	–	6.23 ± 0.97
	lactate production	–	48.13 ± 4.17	5.94 ± 1.48	–
	ATP generation	–	45.36 ± 3.64	2.20 ± 0.40	–
AC PDCs No. 2	glucose uptake	–	27.88 ± 3.18	–	–
	lactate production	–	44.45 ± 3.25	–	–
	ATP generation	–	36.2 ± 9.30	–	–
AC PDCs No. 3	glucose uptake	–	27.49 ± 5.99	–	–
	lactate production	–	22.26 ± 6.49	–	–
	ATP generation	–	20.51 ± 4.56	–	–
AC PDCs No. 4	glucose uptake	–	34.56 ± 4.89	–	–
	lactate production	–	39.40 ± 2.38	–	–
	ATP generation	–	24.47 ± 3.92	–	6.58 ± 1.30
AC PDCs No. 5	glucose uptake	–	54.36 ± 9.38	–	1.95 ± 0.45
	lactate production	–	64.16 ± 5.83	–	6.737186
	ATP generation	–	44.57 ± 4.59	–	6.543977

Abbreviations: PDCs: patients-derived cells; AC: Lung adenocarcinoma; IC_{50}: half maximal inhibitory concentration; ATP: adenosine triphosphate.

4. Discussion

Lung cancer has been one of the foremost fatal human malignancies due to smoking, aging of the population, and environmental pollution. The SCLC and NSCLC are the main subtypes of human lung cancer [22–24]. NSCLC accounts for approximately 80% of all patients suffering from lung cancer, and lung AC is the most common subtype of NSCLC: AC, squamous cell carcinoma, or large cell carcinoma [22–24]. Therefore, this study selected A549 cells, the most commonly used and recognized AC cell line, and PDC lines, using a series of in-vitro or in-vivo methods to detect the antitumor effect of anlotinib. MiRNA is a non-coding RNA playing important roles in gene silencing by acting on the mRNA of a target gene [43,44]. The miRNA is an important component of epigenetic regulation in eukaryotic cells, as well as an

Table 4
The IC_{50} values of anlotinib on AC cells' subcutaneous growth.

Cell lines	Control miRNA	miR-6077	miR-6077 + GLUT1^{Mut}
	IC_{50} values (mg/kg) of anlotinib		
A549	1.63 ± 0.20	0.71 ± 0.2848	1.74 ± 0.40
AC PDCs No. 1	1.92 ± 0.37	0.82 ± 0.21	2.58 ± 0.65
AC PDCs No. 2	1.75 ± 0.81	0.76 ± 0.22	1.44 ± 0.35
AC PDCs No. 3	–	0.86 ± 0.44	–
AC PDCs No. 4	2.05 ± 0.41	0.41 ± 0.05	1.93 ± 0.38
AC PDCs No. 5	1.55 ± 0.42	0.83 ± 0.10	1.52 ± 0.12

Abbreviations: PDCs: patients-derived cells; AC: Lung adenocarcinoma; IC_{50}: half maximal inhibitory concentration.

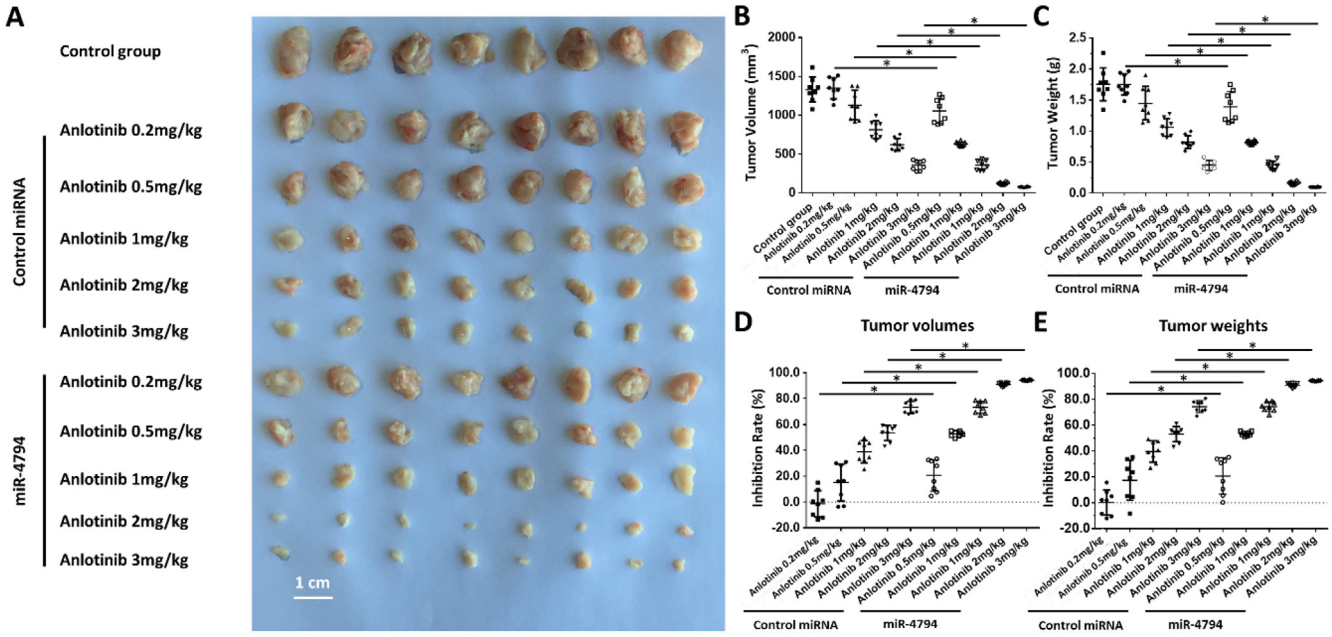

Fig. 4. miR-6077 enhances the sensitivity of A549 cells to anlotinib. A549 cells transfected with control miRNA or miR-6077 were seeded into subcutaneous sites in nude mice to form subcutaneous tumors. Subsequently, these mice received oral administration of anlotinib. The results are shown as (A) images of subcutaneous tumors, (B) tumor volumes of tumor, (C) the inhibition rates of anlotinib according to tumor volumes, (D) tumor weights of tumor, and (E) the inhibition rates of anlotinib according to tumor weights. *P < .05.

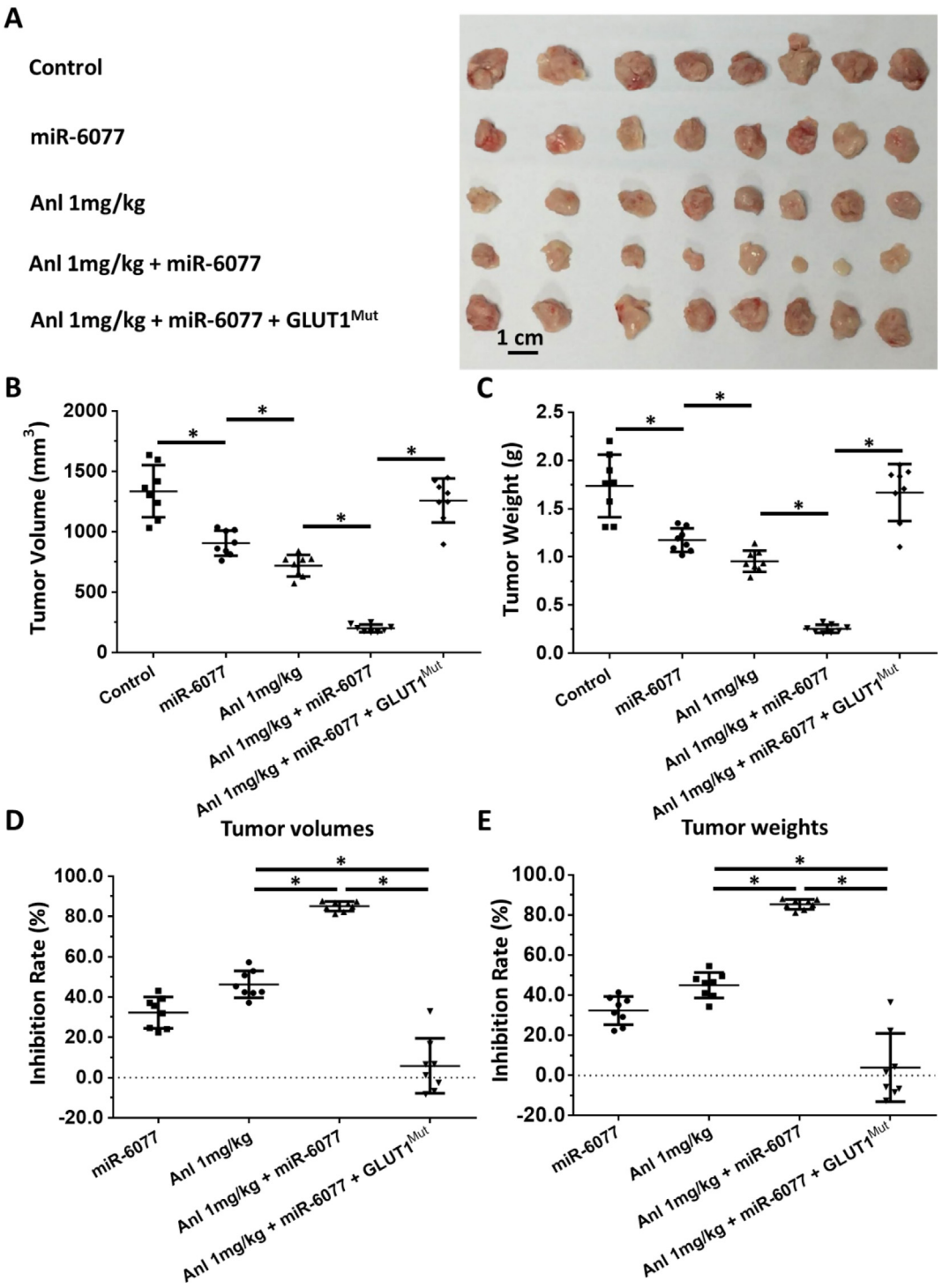

Fig. 5. miR-6077 enhances the sensitivity of A549 cells to anlotinib. A549 cells transfected with control miRNA, miR-6077, or miR-6077 + GLUT1Mut were seeded into subcutaneous sites in nude mice to form subcutaneous tumors. Subsequently, these mice received oral administration of anlotinib. The results are shown as (A) images of subcutaneous tumors, (B) tumor volumes, (C) the inhibition rates of anlotinib according to tumor volumes, (D) tumor weights, and (E) the inhibition rates of anlotinib according to tumor weights. *P < .05.

important regulator of tumor cell proliferation and other related mechanisms [41,42,45]. In addition, the construction and utilization of various viral vectors (i.e., lentivirus, rotavirus, adenoviral vector, etc.) to express full-length sequences of miRNAs in tumor cells and tissues has become a viable strategy for related gene therapy [44,46–51]. In the presence study, the expression vector of miR-6077 was used to prepare lentivirus particles. These particles were used to infect AC cells, leading to a significant sensitization of cells to anlotinib. Moreover, beside miR-6077, Guo et al. (2016) reported that the miRNA-451 could inhibit the proliferation and invasion of glioma cell by downregulating glucose transporter 1 [52]. Ding et al. (2017) reported that the miR-148b inhibits glycolysis in gastric cancer through targeting SLC2A1 (GLUT1) [53]. Santasusagna et al. (2018) reported that the miR-328 could mediate a metabolic shift in colon cancer cells by targeting SLC2A1 (GLUT1) [54]. Yan et al. [80] indicated that the miR-200c could inhibit the proliferation of oral squamous cell carcinoma cells by

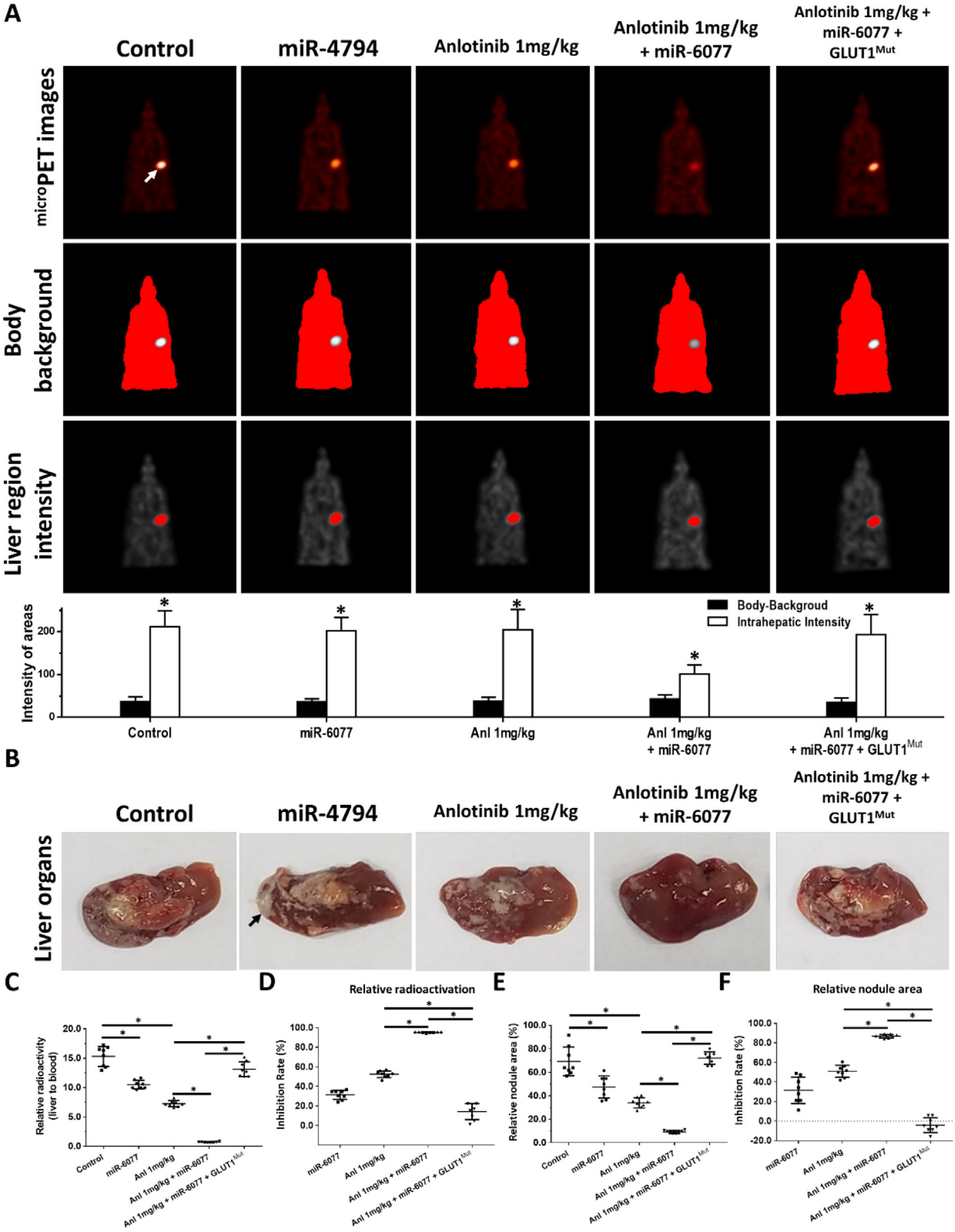

Fig. 6. miR-6077 enhances the sensitivity of A549 cells to anlotinib by targeting GLUT1. A549 cells transfected with control miRNA, miR-6077, or miR-6077 + GLUT1Mut were injected into the livers of nude mice via the hepatic portal vein to mimic the lung cancer-liver migration. Subsequently, the mice received oral administration of anlotinib. The results are shown as (A) images of microPET, (B) images of liver organs with lesions formed by A549 cells, (C) the radio-activation of livers to blood, (D) the inhibition rates of anlotinib on A549 cells according to the radio-activation of liver organs to blood, (E) the relative area of lesions formed by A549 cells in the livers, and (F) the inhibition rates of anlotinib according to the relative area of lesions formed by A549 cells. The arrows were indicated the images of ^{18}F-FDG in nude mice's liver regions (A) or the tumor-lesions formed by AC cells in liver organs of nude mice (B). *P < .05.

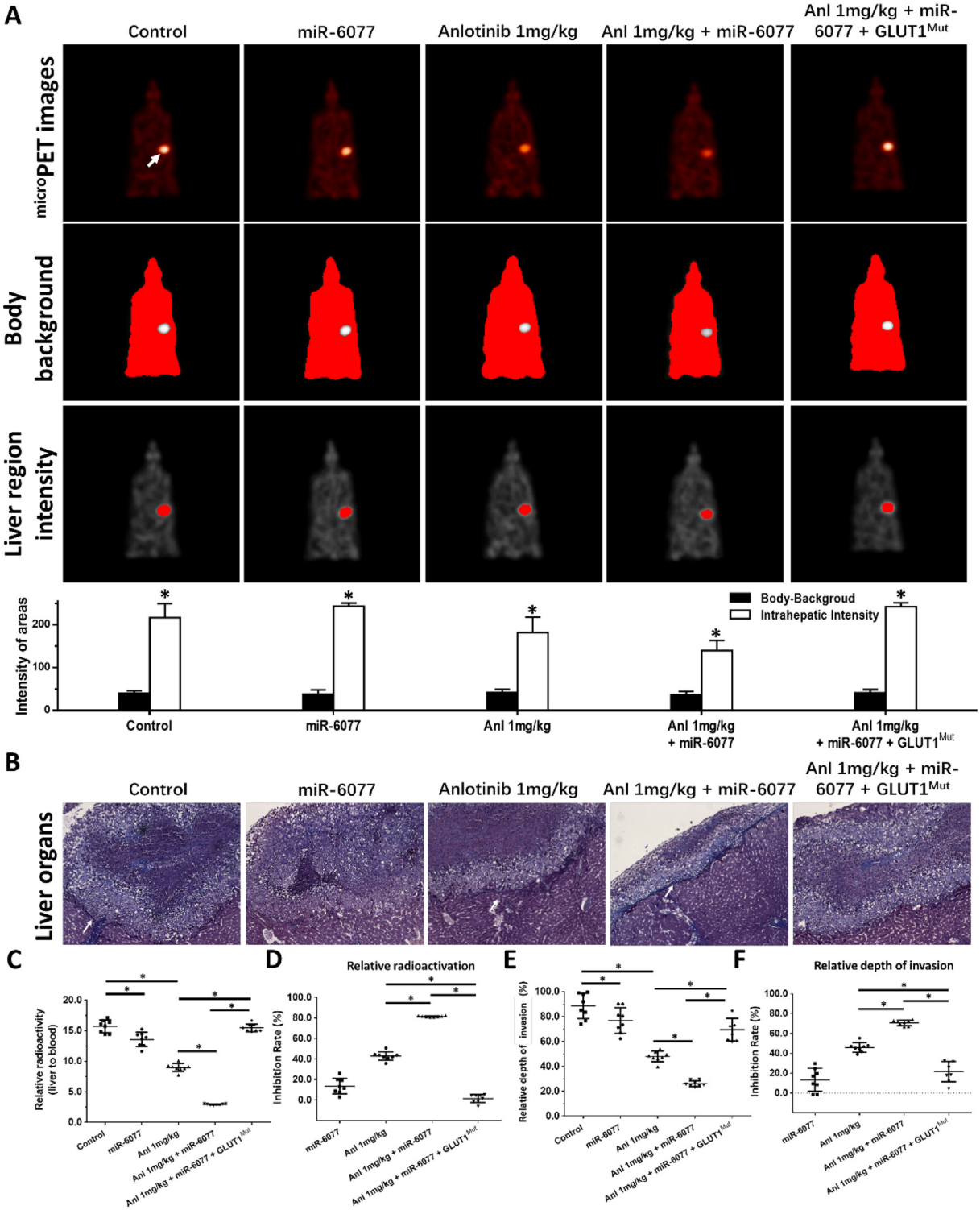

Fig. 7. miR-6077 enhances the sensitivity of A549 cells to anlotinib by targeting GLUT1. A549 cells transfected with control miRNA, miR-6077, or miR-6077 + GLUT1Mut were mixed with hydrogel to adhere onto the surface of livers, mimicking the lung cancer-liver invasion. Subsequently, the mice received oral administration of anlotinib. The results are shown as (A) images of microPET, (B) images of Masson staining of livers with lesions formed by A549 cells, (C) the radio-activation of liver organs to blood, (D) the inhibition rates of anlotinib on A549 cells according to the radio-activation of liver organs to blood, (E) the relative depth of lesions formed by the invasion of A549 cells in the liver, and (F) the inhibition rates of anlotinib according to the relative depth of lesions formed by the invasion of A549 cells in the liver. The arrows were indicated the images of ^{18}F-FDG in nude mice's liver regions (A) or the tumor-lesions formed by AC cells in liver organs of nude mice (B). *P < .05.

targeting Glut1 [55]. These results focus on the miRNA/GLUT1 axis in glioma, gastric cancer, colon cancer or oral squamous cell carcinoma and the study reports the role of miR-6077/GLUT1 axis in lung adenocarcinoma. Interestingly, miRNA could also function as positive regulator of glucose metabolism and Warburg effects. Chen et al. (2019) reported that the miRNA-10a promotes cancer cell proliferation in oral squamous cell carcinoma by upregulating GLUT1 and promoting glucose metabolism [56]. Xu et al. [10] reported that the miR-1204

promotes ovarian squamous cell carcinoma growth by increasing glucose uptake [57]. Therefore, it is valuable to further examine the miRNA targeting on GLUTs and determine whether miRNAs function as a tissues specific feature.

The Warburg effect (aerobic glycolysis) in human cancer cells often exhibits the aberrant metabolism characterized by markedly high levels of glucose-absorption or glycolysis even in the presence of normal oxygen conditions. Moreover, it facilitates alteration of the micro-environment, proliferation, metastasis, or drug resistance by elevating glucose uptake or the accumulation of lactate [58]. Recently, the Warburg effect was shown to be a hallmark of cancer, and a potential target for antitumor treatment [59,60]. There are numerous strategies for inhibiting the Warburg effect in tumor cells: (1) using miRNAs to inhibit the expression of metabolism-related pathways, such as hypoxia-inducible factor or c-MYC [61–67]; or (2) discovering or screening the inhibitor of metabolism-related factors or signaling pathways [68,69]. Among these factors, LDHA is the key enzyme mediating the last step of glycolysis that catalyzes pyruvate into lactate, and is highly expresses in multiple types of human cancer [70–72]. Li et al. reported that miR-30a-5p suppressed the LDHA-mediated Warburg effect and inhibited the growth and metastasis of breast cancer cells [34]. Although LDHA is a major regulator of the Warburg effect and changes in the tumor tissue microenvironment (lactate accumulation), the main cause of the Warburg effect in tumor cells is glucose uptake [71]. In the present study, the expression level of GLUTs in AC specimens was examined. The expression of GLUT1 in tumor tissues was significantly higher than that reported in non-tumor tissues. Among all GLUTs, the expression of GLUT1 in tumor tissues was significantly higher than that observed for other GLUTs. Therefore, GLUT1 may be the most important GLUT in AC. Moreover, overexpression of miR-6077 inhibited the expression of GLUT1, the Warburg effect, and the epithelial-mesenchymal transition process in AC cells. It is established that alteration in the micro-environment of cancer cells is related with the metastasis of cancer cells and especially the development of drug resistance [72]. Therefore, repressing the expression of miR-6077 may be a promising approach for the treatment of AC and it is valuable to examine the detailed mechnisms of miR-6077 on the AC cells' Warburg effects related feature.

Anlotinib is a newly approved molecular targeted agent for the treatment of NSCLC. In the presence study, PDCs were used to examine the sensitivity of cells to anlotinib. Overexpression of miR-6077 enhanced the sensitivity of cells to this agent. Testing the sensitivity of PDCs to anlotinib not only better than using NSCLC cell lines (such as A549), but also assisted in predicting the clinical benefit of therapy with anlotinib to patients. Moreover, this study used a variety of research methods to detect the antitumor activity of anlotinib, including subcutaneous tumor formation and an intrahepatic tumor model. Injection of AC cells via the hepatic portal vein, mimicking the lung cancer-liver metastasis and the invasion of AC cells from the surface of liver into the liver, may quantitatively assess the invasive growth of AC cells [39,73–76]. The metastatic effect of lung cancer in patients is mainly lung cancer brain metastasis, lung cancer liver metastasis and lung cancer bone metastasis [77–79]. This study established related animal models to simulate liver metastasis of lung cancer, and more tumor animal models will be established in the future to simulate lung cancer brain metastasis and lung cancer bone metastasis.

5. Conclusions

In summary, our results indicated that miR-6077 represses the expression of GLUT1 and enhances the sensitivity of patients-derived lung AC cells to anlotinib.

Declaration of Competing Interest

The authors declare no conflict of interest.

Acknowledgments

The authors thank Dr. Yu Cao in Department of Immunology, H. Lee Moffitt Cancer Center & Research Institute, Tampa, FL, 33612, USA for his helpful advices. This work is supported by the Natural Science Foundation of Liaoning Province of China (Grand No. 201602783).

Appendix A. Supplementary data

Supplementary data to this article can be found online at https://doi.org/10.1016/j.cellsig.2019.109391.

References

[1] F. Bray, J. Ferlay, I. Soerjomataram, R.L. Siegel, L.A. Torre, A. Jemal, Global cancer statistics 2018: GLOBOCAN estimates of incidence and mortality worldwide for 36 cancers in 185 countries, CA Cancer J. Clin. 68 (6) (2018) 394–424.
[2] N. Wan, B. Ji, J. Li, J. Jiang, C. Yang, T. Zhang, W. Huang, A pooled meta-analysis of PD-1/L1 inhibitors incorporation therapy for advanced non-small cell lung cancer, Onco. Targets Ther. 12 (2019) 4955.
[3] R. Barnett, Lung cancer, Lancet 390 (2017) 928.
[4] S. Devarakonda, F. Rotolo, M.-S. Tsao, I. Lanc, E. Brambilla, A. Masood, K.A. Olaussen, R. Fulton, S. Sakashita, A. McLeer-Florin, Tumor mutation burden as a biomarker in resected non-small-cell lung cancer, J. Clin. Oncol. 36 (2018) 2995–3006.
[5] R. Ferrara, W.V. Lai, L. Hendriks, J.K. Sabari, C. Caramella, A.J. Plodkowski, D. Halpenny, J.E. Chaft, D. Planchard, G.J. Riely, Impact of baseline steroids on efficacy of programmed cell death-1 and programmed death-ligand 1 blockade in patients with non–small-cell lung cancer, J. Clin. Oncol. 36 (2018) 2872–2878.
[6] Z. Wu, Z. Yang, Y. Dai, Q. Zhu, L.-A. Chen, Update on liquid biopsy in clinical management of non-small cell lung cancer, Onco. Targets Ther. 12 (2019) 5097–5109.
[7] R. Roskoski Jr., Small molecule inhibitors targeting the EGFR/ErbB family of protein-tyrosine kinases in human cancers, Pharmacol. Res. 139 (2019) 395–411.
[8] C. Wei, X. Yao, Z. Jiang, Y. Wang, D. Zhang, X. Chen, X. Fan, C. Xie, J. Cheng, J. Fu, Cordycepin inhibits drug-resistance non-small cell lung cancer progression by activating AMPK signaling pathway, Pharmacol. Res. 144 (2019) 79–89.
[9] X. Wang, H. Yin, H. Zhang, J. Hu, H. Lu, C. Li, M. Cao, S. Yan, L. Cai, NF-κB-driven improvement of EHD1 contributes to erlotinib resistance in EGFR-mutant lung cancers, Cell Death Dis. 9 (4) (2018) 418–429.
[10] L. Xu, X. Meng, N. Xu, W. Fu, H. Tan, L. Zhang, Q. Zhou, J. Qian, S. Tu, X. Li, Gambogenic acid inhibits fibroblast growth factor receptor signaling pathway in erlotinib-resistant non-small-cell lung cancer and suppresses patient-derived xenograft growth, Cell Death Dis. 9 (3) (2018) 262–275.
[11] L. Wang, X. Dong, Y. Ren, J. Luo, P. Liu, D. Su, X. Yang, Targeting EHMT2 reverses EGFR-TKI resistance in NSCLC by epigenetically regulating the PTEN/AKT signaling pathway, Cell Death Dis. 9 (2) (2018) 129–141.
[12] D. Wu, J. Nie, L. Dai, W. Hu, J. Zhang, X. Chen, X. Ma, G. Tian, J. Han, S. Han, Salvage treatment with anlotinib for advanced non-small cell lung cancer, Thorac. Cancer 10 (2019) 1590–1596.
[13] L. Liang, K. Hui, C. Hu, Y. Wen, S. Yang, P. Zhu, L. Wang, Y. Xia, Y. Qiao, W. Sun, Autophagy inhibition potentiates the anti-angiogenic property of multikinase inhibitor anlotinib through JAK2/STAT3/VEGFA signaling in non-small cell lung cancer cells, J. Exp. Clin. Cancer Res. 38 (1) (2019) 71–83.
[14] G. Wang, M. Sun, Y. Jiang, T. Zhang, W. Sun, H. Wang, F. Yin, Z. Wang, W. Sang, J. Xu, Anlotinib, a novel small molecular tyrosine kinase inhibitor, suppresses growth and metastasis via dual blockade of VEGFR2 and MET in osteosarcoma, Int. J. Cancer 145 (4) (2019) 979–993.
[15] Y. Zhao, L. Zhang, Y. Wu, Q. Dai, Y. Zhou, Z. Li, L. Yang, Q. Guo, N. Lu, Selective anti-tumor activity of wogonin targeting the Warburg effect through stablizing p53, Pharmacol. Res. 135 (2018) 49–59.
[16] L. Li, Y. Liang, L. Kang, Y. Liu, S. Gao, S. Chen, Y. Li, W. You, Q. Dong, T. Hong, Transcriptional regulation of the Warburg effect in cancer by SIX1, Cancer Cell 33 (3) (2018) 368-385. e7).
[17] J. Wang, C. Ye, C. Chen, H. Xiong, B. Xie, J. Zhou, Y. Chen, S. Zheng, L. Wang, Glucose transporter GLUT1 expression and clinical outcome in solid tumors: a systematic review and meta-analysis, Oncotarget 8 (10) (2017) 16875–16886.
[18] Z. Dong, X. Zhong, Q. Lei, F. Chen, H. Cui, Transcriptional activation of SIRT6 via FKHRL1/FOXO3a inhibits the Warburg effect in glioblastoma cells, Cell. Signal. 60 (2019) 100–113.
[19] J. Merlin, M. Sato, C. Nowell, M. Pakzad, R. Fahey, J. Gao, N. Dehvari, R.J. Summers, T. Bengtsson, B.A. Evans, The PPARγ agonist rosiglitazone promotes the induction of brite adipocytes, increasing β-adrenoceptor-mediated mitochondrial function and glucose uptake, Cell. Signal. 42 (2018) 54–66.
[20] S. Almahmoud, X. Wang, J.L. Vennerstrom, H.A. Zhong, Conformational studies of glucose transporter 1 (GLUT1) as an anticancer drug target, Molecules 24 (11) (2019) 2159–2175.
[21] M. Roppongi, M. Izumisawa, K. Terasaki, Y. Muraki, M. Shozushima, 18 F-FDG and 11 C-choline uptake in proliferating tumor cells is dependent on the cell cycle in vitro, Ann. Nucl. Med. 33 (4) (2019) 237–243.
[22] R. Roskoski Jr., A. Sadeghi-Nejad, Role of RET protein-tyrosine kinase inhibitors in

the treatment RET-driven thyroid and lung cancers, Pharmacol. Res. 128 (2018) 1–17.
[23] C. Niu, C. Liang, J. Guo, L. Cheng, H. Zhang, X. Qin, Q. Zhang, L. Ding, B. Yuan, X. Xu, Downregulation and growth inhibitory role of FHL1 in lung cancer, Int. J. Cancer 130 (11) (2012) 2549–2556.
[24] J. Mao, L. Ma, Y. Shen, K. Zhu, R. Zhang, W. Xi, Z. Ruan, C. Luo, Z. Chen, X. Xi, Arsenic circumvents the gefitinib resistance by binding to P62 and mediating autophagic degradation of EGFR in non-small cell lung cancer, Cell Death Dis. 9 (10) (2018) 963–977.
[25] J. Wang, Y. Zhao, Q. Wang, L. Zhang, J. Shi, Z. Wang, Y. Cheng, J. He, Y. Shi, H. Yu, Prognostic factors of refractory NSCLC patients receiving anlotinib hydrochloride as the third-or further-line treatment, Cancer Biol. Med. 15 (4) (2018) 443–451.
[26] D. Ma, H. Jia, M. Qin, W. Dai, T. Wang, E. Liang, G. Dong, Z. Wang, Z. Zhang, F. Feng, MiR-122 induces radiosensitization in non-small cell lung cancer cell line, Int. J. Mol. Sci. 16 (9) (2015) 22137–22150.
[27] Q. Ji, X. Xu, L. Li, S.B. Goodman, W. Bi, M. Xu, Y. Xu, Z. Fan, W.J. Maloney, Q. Ye, miR-216a inhibits osteosarcoma cell proliferation, invasion and metastasis by targeting CDK14, Cell Death Dis. 8 (10) (2017) (e3103–3113).
[28] Y. Liang, X. Xu, T. Wang, Y. Li, W. You, J. Fu, Y. Liu, S. Jin, Q. Ji, W. Zhao, The EGFR/miR-338-3p/EYA2 axis controls breast tumor growth and lung metastasis, Cell Death Dis. 8 (7) (2017) e2928–e2939.
[29] T. Makabe, E. Arai, T. Hirano, N. Ito, Y. Fukamachi, Y. Takahashi, A. Hirasawa, W. Yamagami, N. Susumu, D. Aoki, Genome-wide DNA methylation profile of early-onset endometrial cancer: its correlation with genetic aberrations and comparison with late-onset endometrial cancer, Carcinogenesis 40 (2019) 611–623.
[30] C. Demuth, A. Winther-Larsen, A.T. Madsen, P. Meldgaard, B.S. Sorensen, A method for treatment monitoring using circulating tumour DNA in cancer patients without targetable mutations, Oncotarget 9 (57) (2018) 31066–31076.
[31] F. Guan, R. Ding, Q. Zhang, W. Chen, F. Li, L. Long, W. Li, L. Li, D. Yang, L. Xie, WX-132-18B, a novel microtubule inhibitor, exhibits promising anti-tumor effects, Oncotarget 8 (42) (2017) 71782–71796.
[32] Y. Wang, Z. Tang, Anovel long-sustaining system of apatinib for long-term inhibition of the proliferation of hepatocellular carcinoma cells, Onco. Targets Ther. 11 (2018) 8529–8541.
[33] H. Xie, S. Tian, H. Yu, X. Yang, J. Liu, H. Wang, F. Feng, Z. Guo, A new apatinib microcrystal formulation enhances the effect of radiofrequency ablation treatment on hepatocellular carcinoma, Onco. Targets Ther. 11 (2018) 3257–3265.
[34] L. Li, L. Kang, W. Zhao, Y. Feng, W. Liu, T. Wang, H. Mai, J. Huang, S. Chen, Y. Liang, et al., Cancer Lett. 400 (2017) 89–98.
[35] H. Jia, Q. Yang, T. Wang, Y. Cao, Q.-y. Jiang, H.-w. Sun, M.-x. Hou, Y.-p. Yang, F. Feng, Rhamnetin induces sensitization of hepatocellular carcinoma cells to a small molecular kinase inhibitor or chemotherapeutic agents, Biochim. Biophys. Acta 1860 (7) (2016) 1417–1430.
[36] L. An, D.-D. Li, H.-X. Chu, Q. Zhang, C.-L. Wang, Y.-H. Fan, Q. Song, H.-D. Ma, F. Feng, Q.-C. Zhao, Terfenadine combined with epirubicin impedes the chemo-resistant human non-small cell lung cancer both in vitro and in vivo through EMT and notch reversal, Pharmacol. Res. 124 (2017) 105–115.
[37] X. Xu, Z. Fan, C. Liang, L. Li, L. Wang, Y. Liang, J. Wu, S. Chang, Z. Yan, Z. Lv, A signature motif in LIM proteins mediates binding to checkpoint proteins and increases tumour radiosensitivity, Nat. Commun. 8 (2017) 14059–14072.
[38] L. Wei, Y. Lun, X. Zhou, S. He, L. Gao, Y. Liu, Z. He, B. Li, C. Wang, Novel urokinase-plasminogen activator inhibitor SPINK13 inhibits growth and metastasis of hepatocellular carcinoma in vivo, Pharmacol. Res. 143 (2019) 73–85.
[39] D. Meng, M. Lei, Y. Han, D. Zhao, X. Zhang, Y. Yang, R. Liu, MicroRNA-645 targets urokinase plasminogen activator and decreases the invasive growth of MDA-MB-231 triple-negative breast cancer cells, Onco. Targets Ther. 11 (2018) 7733–7743.
[40] Y. Zhang, D. Li, Q. Jiang, S. Cao, H. Sun, Y. Chai, X. Li, T. Ren, R. Yang, F. Feng, Novel ADAM-17 inhibitor ZLDI-8 enhances the in vitro and in vivo chemotherapeutic effects of Sorafenib on hepatocellular carcinoma cells, Cell Death Dis. 9 (7) (2018) 743–755.
[41] R. Li, M. Qiao, X. Zhao, J. Yan, X. Wang, Q. Sun, MiR-20a-3p regulates TGF-β1/Survivin pathway to affect keratinocytes proliferation and apoptosis by targeting SFMBT1 in vitro, Cell. Signal. 49 (2018) 95–104.
[42] K. Sen, D. Bhattacharyya, A. Sarkar, J. Das, N. Maji, M. Basu, Z. Ghosh, T.C. Ghosh, Exploring the major cross-talking edges of competitive endogenous RNA networks in human Chronic and Acute Myeloid Leukemia, Biochim. Biophys. Acta Gen. Subj. 1862 (9) (2018) 1883–1892.
[43] A. Garcia-Concejo, A. Jimenez-Gonzalez, R.E. Rodriguez, Opioid and notch signaling pathways are reciprocally regulated through miR-29a and miR-212 expression, Biochim. Biophys. Acta Gen. Subj. 1862 (12) (2018) 2605–2612.
[44] L. Liu, Y.-C. Tian, G. Mao, Y.-G. Zhang, L. Han, MiR-675 is frequently overexpressed in gastric cancer and enhances cell proliferation and invasion via targeting a potent anti-tumor gene PITX1, Cell. Signal. 62 (2019) 109352–109362.
[45] C. Zhang, C. Chang, H. Gao, Q. Wang, F. Zhang, C. Xu, MiR-429 regulates rat liver regeneration and hepatocyte proliferation by targeting JUN/MYC/BCL2/CCND1 signaling pathway, Cell. Signal. 50 (2018) 80–89.
[46] D.H. Kim, H. Khan, H. Ullah, S.T. Hassan, K. Šmejkal, T. Efferth, M.F. Mahamoodally, S. Xu, S. Habtemariam, R. Filosa, MicroRNA targeting by quercetin in cancer treatment and chemoprotection, Pharmacol. Res. 147 (2019) 104346–104359.
[47] V. Sanchez, F. Golyardi, D. Mayaki, R. Echavarria, S. Harel, J. Xia, S.N. Hussain, Negative regulation of angiogenesis by novel micro RNAs, Pharmacol. Res. 139 (2019) 173–181.
[48] Y. Wang, K. Wang, Z. Hu, H. Zhou, L. Zhang, H. Wang, G. Li, S. Zhang, X. Cao, F. Shi, MicroRNA-139-3p regulates osteoblast differentiation and apoptosis by targeting ELK1 and interacting with long noncoding RNA ODSM, Cell Death Dis. 9 (11) (2018) 1107–1123.
[49] D. Liu, L. Zhong, Z. Yuan, J. Yao, P. Zhong, J. Liu, S. Yao, Y. Zhao, L. Liu, M. Chen, miR-382-5p modulates the ATRA-induced differentiation of acute promyelocytic leukemia by targeting tumor suppressor PTEN, Cell. Signal. 54 (2019) 1–9.
[50] K. Kyriakopoulou, E. Kefali, Z. Piperigkou, H. Bassiony, N.K. Karamanos, Advances in targeting epidermal growth factor receptor signaling pathway in mammary cancer, Cell. Signal. 51 (2018) 99–109.
[51] H. Xiong, T. Yan, W. Zhang, F. Shi, X. Jiang, X. Wang, S. Li, Y. Chen, C. Chen, Y. Zhu, miR-613 inhibits cell migration and invasion by downregulating Daam1 in triple-negative breast cancer, Cell. Signal. 44 (2018) 33–42.
[52] H. Guo, Y. Nan, Y. Zhen, Y. Zhang, L. Guo, K. Yu, Q. Huang, Y. Zhong, miRNA-451 inhibits glioma cell proliferation and invasion by downregulating glucose transporter 1, Tumour Biol. 37 (2016) 13751–13761.
[53] X. Ding, J. Liu, T. Liu, Z. Ma, D. Wen, L. Zhu, miR-148b inhibits glycolysis in gastric cancer through targeting SLC2A1, Cancer Med. 6 (2017) 1301–1310.
[54] S. Santasusagna, I. Moreno, A. Navarro, C. Muñoz, F. Martinez, R. Hernández, J.J. Castellano, M. Monzo, miR-328 mediates a metabolic shift in colon cancer cells by targeting SLC2A1/GLUT1, Clin. Transl. Oncol. 20 (2018) 1161–1167.
[55] Y. Yan, F. Yan, Q. Huang, MiR-200c inhibited the proliferation of oral squamous cell carcinoma cells by targeting Akt pathway and its downstream Glut1, Arch. Oral Biol. 96 (2018) 52–57.
[56] Y.H. Chen, Y. Song, Y.L. Yu, W. Cheng, X. Tong, miRNA-10a promotes cancer cell proliferation in oral squamous cell carcinoma by upregulating GLUT1 and promoting glucose metabolism, Oncol. Lett. 17 (2019) 5441–5446.
[57] J. Xu, X. Gu, X. Yang, Y. Meng, MiR-1204 promotes ovarian squamous cell carcinoma growth by increasing glucose uptake, Biosci. Biotechnol. Biochem. (2018) 1–6.
[58] H. Xiao, J. Wang, W. Yan, Y. Cui, Z. Chen, X. Gao, X. Wen, J. Chen, GLUT1 regulates cell glycolysis and proliferation in prostate cancer, Prostate 78 (2) (2018) 86–94.
[59] W. Yu, Z. Yang, R. Huang, Z. Min, M. Ye, SIRT6 promotes the Warburg effect of papillary thyroid cancer cell BCPAP through reactive oxygen species, Onco. Targets Ther. 12 (2019) 2861–2868.
[60] Z. Wang, Q. Zhou, A. Li, W. Huang, Z. Cai, W. Chen, Extracellular matrix protein 1 (ecM1) is associated with carcinogenesis potential of human bladder cancer, Onco. Targets Ther. 12 (2019) 1423–1432.
[61] L. Penolazzi, G. Bonaccorsi, R. Gafà, N. Ravaioli, D. Gabriele, C. Bosi, G. Lanza, P. Greco, R. Piva, SLUG/HIF1-α/miR-221 regulatory circuit in endometrial cancer, Gene 711 (2019) 143938–143943.
[62] D. Zhang, Z. Shi, M. Li, J. Mi, Hypoxia-induced miR-424 decreases tumor sensitivity to chemotherapy by inhibiting apoptosis, Cell Death Dis. 5 (6) (2014) e1301–e1308.
[63] B. Majem, A. Parrilla, C. Jiménez, L. Suárez-Cabrera, M. Barber, A. Marín, J. Castellví, G. Tamayo, G. Moreno-Bueno, J. Ponce, MicroRNA-654-5p suppresses ovarian cancer development impacting on MYC, WNT and AKT pathways, Oncogene 38 (32) (Aug 2019) 6035–6050, https://doi.org/10.1038/s41388-019-0860-0 (Epub 2019 Jul 5).
[64] Z. Liang, Z. Liu, C. Cheng, H. Wang, X. Deng, J. Liu, C. Liu, Y. Li, W. Fang, VPS33B interacts with NESG1 to modulate EGFR/PI3K/AKT/c-Myc/P53/miR-133a-3p signaling and induce 5-fluorouracil sensitivity in nasopharyngeal carcinoma, Cell Death Dis. 10 (4) (2019) 305–320.
[65] F. Yu, G. Pang, G. Zhao, ANRIL acts as onco-lncRNA by regulation of microRNA-24/c-Myc, MEK/ERK and Wnt/β-catenin pathway in retinoblastoma, Int. J. Biol. Macromol. 128 (2019) 583–592.
[66] F. Li, A. Wei, L. Bu, L. Long, W. Chen, C. Wang, C. Zhao, L. Wang, Procaspase-3-activating compound 1 stabilizes hypoxia-inducible factor 1α and induces DNA damage by sequestering ferrous iron, Cell Death Dis. 9 (10) (2018) 1025–1039.
[67] D. Bashash, M. Sayyadi, A. Safaroghli-Azar, N. Sheikh-Zeineddini, N. Riyahi, M. Momeny, Small molecule inhibitor of c-Myc 10058-F4 inhibits proliferation and induces apoptosis in acute leukemia cells, irrespective of PTEN status, Int. J. Biochem. Cell Biol. 108 (2019) 7–16.
[68] H. Sawayama, Y. Ogata, T. Ishimoto, K. Mima, Y. Hiyoshi, M. Iwatsuki, Y. Baba, Y. Miyamoto, N. Yoshida, H. Baba, Glucose transporter 1 regulates the proliferation and cisplatin sensitivity of esophageal cancer, Cancer Sci. 110 (5) (2019) 1705–1714.
[69] C. Wu, N. Gupta, Y.-H. Huang, H.-F. Zhang, A. Alshareef, A. Chow, R. Lai, Oxidative stress enhances tumorigenicity and stem-like features via the activation of the Wnt/β-catenin/MYC/Sox2 axis in ALK-positive anaplastic large-cell lymphoma, BMC Cancer 18 (1) (2018) 361–371.
[70] M. Manerba, M. Govoni, I. Manet, A. Leale, A. Comparone, G. Di Stefano, Metabolic activation triggered by cAMP in MCF-7 cells generates lethal vulnerability to combined oxamate/etomoxir, Biochim. Biophys. Acta Gen. Subj. 1863 (7) (2019) 1177–1186.
[71] W. Zhang, G. Wang, Z.-G. Xu, H. Tu, F. Hu, J. Dai, Y. Chang, Y. Chen, Y. Lu, H. Zeng, Lactate is a natural suppressor of RLR signaling by targeting MAVS, Cell 178 (2019) 176–189.
[72] P.B. Ancey, C. Contat, E. Meylan, Glucose transporters in cancer–from tumor cells to the tumor microenvironment, FEBS J. 285 (16) (2018) 2926–2943.
[73] Z. Shao, Y. Li, W. Dai, H. Jia, Y. Zhang, Q. Jiang, Y. Chai, X. Li, H. Sun, R. Yang, ETS-1 induces Sorafenib-resistance in hepatocellular carcinoma cells via regulating transcription factor activity of PXR, Pharmacol. Res. 135 (2018) 188–200.
[74] Y. Chen, Q. Zeng, X. Liu, J. Fu, Z. Zeng, Z. Zhao, Z. Liu, W. Bai, Z. Dong, H. Liu, LINE-1 ORF-1p enhances the transcription factor activity of pregnenolone X receptor and promotes sorafenib resistance in hepatocellular carcinoma cells, Cancer Manag. Res. 10 (2018) 4421–4438.
[75] D. Meng, H. Lei, X. Zheng, Y. Han, R. Sun, D. Zhao, R. Liu, A temperature-sensitive phase-change hydrogel of tamoxifen achieves the long-acting antitumor activation on breast cancer cells, Onco. Targets Ther. 12 (2019) 3919–3931.

[76] D. Meng, M. Meng, A. Luo, X. Jing, G. Wang, S. Huang, M. Luo, S. Shao, X. Zhao, R. Liu, Effects of VEGFR1 + hematopoietic progenitor cells on pre-metastatic niche formation and in vivo metastasis of breast cancer cells, J. Cancer Res. Clin. Oncol. 145 (2) (2019) 411–427.

[77] K. Dong, W. Liang, S. Zhao, M. Guo, Q. He, C. Li, H. Song, J. He, X. Xia, EGFR-TKI plus brain radiotherapy versus EGFR-TKI alone in the management of EGFR-mutated NSCLC patients with brain metastases, Transl. Lung Cancer Res. 8 (2019) 268–279.

[78] D. Chen, T. Chu, Q. Chang, Y. Zhang, L. Xiong, R. Qiao, J. Teng, B. Han, R. Zhong, The relationship between preliminary efficacy and prognosis after first-line EGFR tyrosine kinase inhibitor (EGFR-TKI) treatment of advanced non-small cell lung cancer, Ann. Transl. Med. 7 (2019) 195.

[79] X.Y. Yang, J.J. Liao, W.R. Xue, FMNL1 down-regulation suppresses bone metastasis through reducing TGF-β1 expression in non-small cell lung cancer (NSCLC), Biomed. Pharmacother. 117 (2019) 109126.

[80] Y. Yan, F. Yan, Q. Huang, MiR-200c inhibited the proliferation of oral squamous cell carcinoma cells by targeting Akt pathway and its downstream Glut1, Arch. Oral. Biol. 96 (Dec 2018) 52–57, https://doi.org/10.1016/j.archoralbio.2018.06.003 (Epub 2018 Jun 6).